Adaptation of an Animal Territory Model to Street Gang Spatial Patterns in Los Angeles

Laura M. Smith[1], Andrea L. Bertozzi[1], P. Jeffrey Brantingham[2], George E. Tita[3] and Matthew Valasik[3]

[1]UCLA Mathematics Department, 520 Portola Plaza , Box 951555, Los Angeles, CA 90095-1555,
[2]UCLA Anthropology Department, 375 Portola Plaza , 341 Haines Hall, Box 951553, Los Angeles, CA 90095-1553,
[3]UCI Department of Criminology, Law and Society, 2340 Social Ecology II, Irvine, CA 92697-7080,

February 15, 2012

Abstract

Territorial animals and street gangs exhibit similar behavioral characteristics. Both organize themselves around a home base and mark their territories to distinguish claimed regions. Moorcroft et al. model the formation of territories and spatial distributions of coyote packs and their markings in [24]. We modify this approach to simulate gang dynamics in the Hollenbeck policing division of eastern Los Angeles. We incorporate important geographical features from the region that would inhibit movement, such as rivers and freeways. From the gang and marking densities created by this method, we create a rivalry network from overlapping territories and compare the graph to both the observed network and those constructed through other methods. Data on the locations of where gang members have been observed is then used to analyze the densities created by the model.

1 Introduction

Street gangs have a long history in Los Angeles [25, 34] and are major contributors to violent acts in the region [9, 27, 28]. Gangs compete to secure both instrumental (e.g., money, drugs, space) and expressive (e.g., reputation, power) resources, often causing a partitioning of the city into gang territories [31]. Disputes over spatial resources may lead to violence and acts of retribution, augmenting or creating a rivalry between gangs [9, 32]. One common method for a gang to mark its territory is through the use of graffiti [1, 8, 22]. This is analogous to territorial animals, such as wolves, claiming spatial regions via scent marking or other means [26]. Several models have recently been proposed to describe the territorial behavior of species as diverse as wolves [5, 7, 20, 21, 37], coyotes [23, 24], killer wasps [10], chimpanzees [36], and birds [19].

This paper examines the formation of gang territories and territorial marking using the approach given in [24] based on a system of partial differential equations. Section 2 describes this approach for coyotes and its relationship to gangs. Section 3 provides information on Hollenbeck, the eastern policing division of Los Angeles, which is the case study for which this model is applied. The implementation details are given in

Section 4, and a description of the data sets are provided in Section 5. The results follow in Section 6. Section 7 concludes the paper with a discussion of the model implications.

2 Modeling Street Gangs

This paper develops a model to describe the equilibrium densities of gangs and gang graffiti. Gang graffiti marks the boundaries of contested regions claimed by multiple gangs, which may make these areas more prone to violence. The boundaries of gang territories change over time as new gangs emerge and older gangs cease to exist. By creating a flexible model that can incorporate these fluctuations, theories can be tested to investigate the system dynamics given certain changes [11, 15].

2.1 Existing Gang Models

Several models have recently been proposed for analyzing various gang behaviors. Retaliatory behavior among gangs has been simulated via self-exciting point processes [12, 29]. These methods focus on the temporal aspect of gang violence. Using this gang characteristic of retaliation, attempts have been made to fill in the missing data of which gang is responsible for a crime [30]. From a different perspective, the authors of [3] use an approach from epidemiology to simulate membership in gangs.

A recent bottom-up approach examines the formation of rivalries. In [16], the authors propose an agent-based model that is coupled to a rivalry network. A node of the network represents a geographic position that is the central location to a gang's activities known as a *set space* [28, 33]. An edge in the network is present if there is a rivalry between the two gangs. In this stochastic model, agents move about the city and interact with members of other gangs. Once two gang members of different gangs cross paths, the weight of the edge between their two respective nodes is increased. This edge weight directly impacts the directional decisions the agents make, which is biased towards their home set space and away from rival gangs' set spaces and selected from a von Mises distribution [18]. Additionally, geographic boundaries in the region are incorporated into this model to restrict movement across rivers and large freeways. The model we propose here will include these geographic boundaries and compare the resulting rivalry network with those obtained in [16].

The Lotka-Volterra competition model has been used to analyze the creation of territorial boundaries between two gangs in [6]. Through this approach, the authors examined the locations of violent interactions with respect to the theoretical boundary between the two gangs and concluded that violence typically clusters about this dividing curve. Another model uses graffiti as the mechanism for interactions between gang members and analyzes the circumstances under which territories are formed [4]. Both of these methods focus only on situations with two gangs. In order to fully examine a system of twenty-nine active gangs in the Hollenbeck policing division of Los Angeles, we will consider another approach taken from ecology.

2.2 Territorial Animal Models

Many species exhibit territorial behavior, where individuals and/or groups are willing to defend space they currently hold from incursions by members of the same species (intraspecific competition) or other species (interspecific competition). These behavioral

characteristics are similar to those of street gangs which use violence to control local drug markets or simply defend their neighborhood from outsiders. For this reason, we consider existing models of territorial animals. The paper [17] provides a review of partial differential equation models proposed for studying the spatial distributions of species. Some approaches include diffusion models, diffusion with drift and convection models, biased random motion models, models with aggregation or repulsion that depends on the current organism density, and models that depend on environmental features. Additionally, reaction-diffusion and predator-prey models incorporate competition into the system.

Two competing groups might never physically meet, yet still have defined territories. Coyotes and wolves are animals that exhibit territorial behavior through raised leg urination. When an individual comes in contact with a marking from a different pack, the animal increases its own urination and moves towards its home den located on the interior of its territory [20]. This avoidance of markings has been incorporated into wolf [5, 7, 20, 21, 37] and coyote models [23, 24] through a coupled system of partial differential equations for both the pack densities and the marking densities. The most recent of these models [24] also includes a mechanism to avoid areas where the terrain is steep, and it is this model that we will modify to examine the spatial behaviors of street gangs.

2.3 The Proposed Gang Behavioral Model

The description of the behavioral characteristics of territorial animals is analogous to gangs in several ways. First, both gangs and territorial animals have distinctly claimed areas that are well-established. Both use markings to inform members of both their own group as well as other groups of territorial boundaries. Individuals may respond to markings of other groups by increasing their own marking density and by biasing their movement towards their respective den site or set space.

The particular model of interest in [24] is called, "steep terrain avoidance plus conspecific avoidance (STA+CA)." It is given by solving the following non-dimensionalized system to steady-state:

$$\frac{du^{(i)}}{dt} = \Delta u^{(i)} - \nabla \cdot \left[\beta \mathbf{x}_i u^{(i)} \sum_{j \neq i}^{n} p^{(j)} \right] + \nabla \cdot \left[\alpha u^{(i)} \nabla z \right] \tag{1}$$

$$\frac{dp^{(i)}}{dt} = u^{(i)} \left[1 + m \sum_{j \neq i}^{n} p^{(j)} \right] - p^{(i)}, \tag{2}$$

where for a given pack i, $u^{(i)}(x, y)$ is the expected population density, $p^{(i)}(x, y)$ is the expected marking density, and $\mathbf{x}_i$ is the unit vector to the home den site (or set space for gangs) from the current location. The parameters β, m, and α represent the strengths to avoid markings, to increase one's own markings, and to avoid steep terrain, respectively. This system also has the boundary conditions on $\partial\Omega$

$$0 = \left[\nabla u^{(i)} - \beta \mathbf{x}_i u^{(i)} \sum_{j \neq i}^{n} p^{(j)} + \alpha u^{(i)} \nabla z \right] \cdot \vec{\mathbf{n}}, \tag{3}$$

where $\vec{\mathbf{n}}$ is the outward unit normal vector.

The system in Equations (1) and (2) models population densities and marking densities for a set of gangs or pack of coyotes. More specifically, the term $\Delta u^{(i)}$ describes

random motion of individuals. Since gangs typically avoid the territories of other gangs [2, 22] unless they are conducting a violent raid, they are more likely to return towards their set space when confronted by another gang's tags. This behavior is represented by the term $-\nabla \cdot \left[\beta \mathbf{x}_i u^{(i)} \sum_{j \neq i}^{n} p^{(j)}\right]$, where individuals that come in contact with any markings that are not of their own gang move in the direction towards home, $\mathbf{x}_i$. Equation (2) describes the process by which individuals increase their production of markings after discovering another gang's markings.

The $z(x, y)$ in the model is the elevation of the terrain for coyotes, but we use this term to incorporate other spatial features. We first determine geographical landmarks that could inhibit movement across them, such as rivers, freeways, and major roads. These features are not impassible, but there are limited bridges and underpasses available. We then divide the area into regions separated by these features. Letting z be zero where there is a landmark and one otherwise, this gives a "steep terrain" that gang members will avoid. Territory is therefore incorporated into the movement dynamics through the final term in Equation (1), $\nabla \cdot \left[\alpha u^{(i)} \nabla z\right]$.

This partial differential equation approach has many features similar to the agent-based model proposed in [16]. Both models incorporate the geography as semi-permeable boundaries. Additionally, individuals engage in random movement, but have a bias towards their home set space. In the supplementary material for [24], the authors derive the model given in Equations (1) and (2) by using a von Mises distribution for the advection term. Thus, both models utilize the von Mises distribution to generate directionally biased motion. One major difference between the two methods is that the model proposed in this paper is deterministic, whereas the agent-based approach is stochastic. Due to the similarities in these models, we will also use Hollenbeck as the case study and compare the results to those given in [16].

3 Street Gangs in Hollenbeck

Eastern Los Angeles is plagued by gang violence. Hollenbeck, a policing division of the Los Angeles Police Department, is home to twenty-nine active Latino street gangs in only 15.2 square miles [28, 34]. Due to the geography of the area, the rivalries among the gangs in this region are generally restricted to Hollenbeck. Most of the rivalries and disputes among these gangs is linked to neighborhood-based territoriality rather than drugs or other conflicts.

To examine the structure of the rivalries in Hollenbeck, we view a graph that is embedded in space with nodes representing the set spaces of the gangs. If a rivalry exists between two gangs, then an edge is present between the two respective nodes. Among the twenty-nine gangs in Hollenbeck, there are sixty-nine observed rivalries. This observed network has been examined in [16, 28, 34]. The authors of these papers argue that the structure of this network is highly dependent on the geography of the region and the highways and rivers that pass through the area. Five major freeways, I-5, I-10, I-710, CA-60, and US-101, divide Hollenbeck into many sections. Figure 1 shows the spatially embedded rivalry network and the features that partition the region. It is clear that these physical boundaries impact the rivalry structure by limiting the number of rivalries between gangs in separate sections.

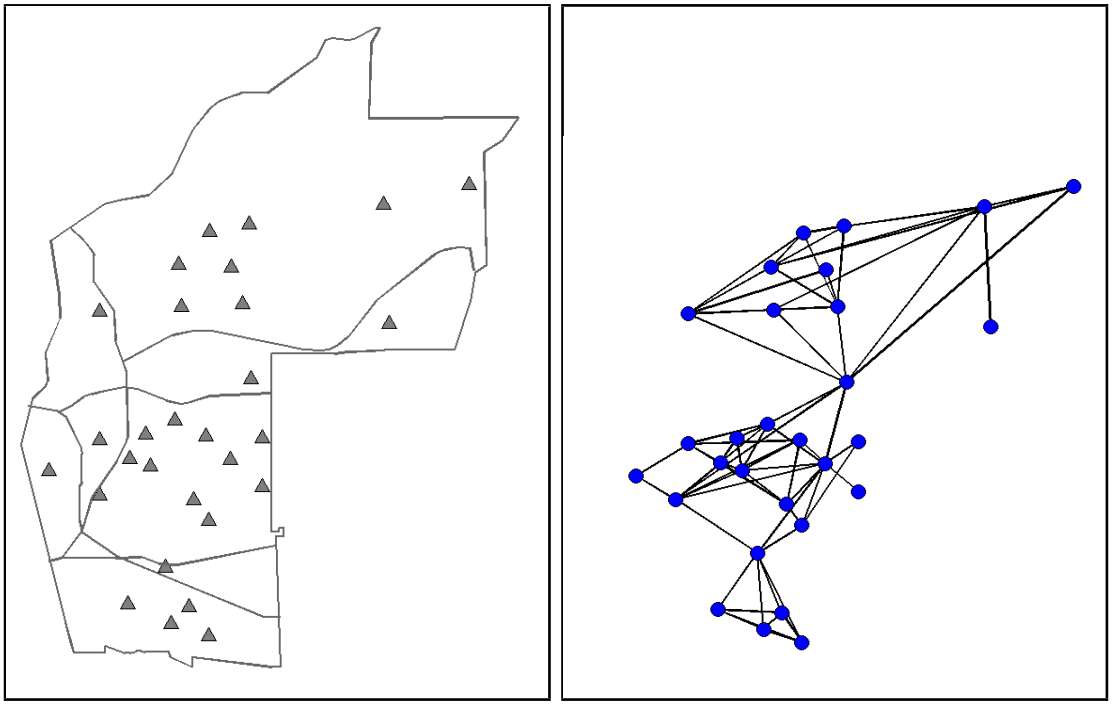

Figure 1: Set spaces embedded in Hollenbeck (Left) and the corresponding observed rivalry network (Right). Each solid triangle on the left and solid circle on the right gives the location of a gang's set space. The faint curves (Left) show the major roads and rivers that pass through the region, impacting the rivalry structure. The policing division boundary is also included as the bottom and right boundaries. The observed network from [28] is displayed on the right, where an edge between two gangs indicates an existing rivalry between the gangs.

4 Implementation Details

For the G gangs, the model consists of a coupled system with $2G$ differential equations. We implemented this system by using finite differences and solving until steady-state. For each time step Δt, we loop through all of the gangs, updating first the $u^{(k)}$ and then $p^{(k)}$. For initialization, $u^{(k)}$ is set to be zero everywhere except at the location of the k^{th} set space, where it has the value one. Alternatively, $p^{(k)}$ is intialized to be $\frac{1}{NM}$ everywhere, where the grid is $N \times M$. The discretized equation for the interior of $u^{(k)}$ at time $n+1$ is given by

$$\begin{aligned}
\frac{u_{i,j}^{(k),n+1} - u_{i,j}^{(k),n}}{\Delta t} &= \frac{1}{(\Delta x)^2}\left(u_{i+1,j}^{(k),n} - 2u_{i,j}^{(k),n} + u_{i-1,j}^{(k),n}\right) \\
&+ \frac{1}{(\Delta y)^2}\left(u_{i,j+1}^{(k),n} - 2u_{i,j}^{(k),n} + u_{i,j-1}^{(k),n}\right) \\
&- \frac{\beta}{2\Delta x}\left(u_{i+1,j}^{(k),n}\ x_{i+1,j}^{(k)} \sum_{l\neq k} p_{i+1,j}^{(l),n} - u_{i-1,j}^{(k),n}\ x_{i-1,j}^{(k)} \sum_{l\neq k} p_{i-1,j}^{(l),n}\right) \\
&- \frac{\beta}{2\Delta y}\left(u_{i,j+1}^{(k),n}\ y_{i,j+1}^{(k)} \sum_{l\neq k} p_{i,j+1}^{(l),n} - u_{i,j-1}^{(k),n}\ y_{i,j-1}^{(k)} \sum_{l\neq k} p_{i,j-1}^{(l),n}\right) \\
&+ \frac{\alpha}{\Delta x}\left(u_{i+1,j}^{(k),n}\ \nabla_x\ z_{i+1,j} - u_{i,j}^{(k),n}\ \nabla_x\ z_{i,j}\right)
\end{aligned}$$

$$+\frac{\alpha}{\Delta y}\left(u_{i,j+1}^{(k),n}\ \nabla_y\ z_{i,j+1} - u_{i,j}^{(k),n}\ \nabla_y\ z_{i,j}\right).$$

The boundary of $u^{(k)}$ is updated using first order Neumann boundary conditions. Given this update of $u^{(k)}$, we then update both the interior and boundary of $p^{(k)}$ as

$$\frac{p_{i,j}^{(k),n+1} - p_{i,j}^{(k),n}}{\Delta t} \quad = \quad u_{i,j}^{(k),n+1}\left(1 + m\ \sum_{l\neq k} p_{i,j}^{(l),n}\right) - p_{i,j}^{(k),n+1}.$$

After this update, we ensure that $p^{(k)}$ is still a density that sums to one. After obtaining our final estimates for the gang and marking densities, we determine that a rivalry exists between two gangs if the regions where densities are non-negligible sufficiently overlap.

5 The Data Sets

In order to test the algorithm, we will use two different data sets. The first covers the years 1999 to 2002 and gives the locations of violence between two gangs. We only use the 340 events where both the suspect and victim gang are known and both are also in the set of twenty-nine Hollenbeck gangs. In [6], the authors compared the locations of events relative to the theoretical midline boundary between gangs. They concluded that violent interactions frequently cluster about this line. From this analysis, we should expect a higher density of violent events near the boundaries of territories, but also in areas where there is an increase in graffiti. For our model, this is where the markings, $p^{(i)}$, have a high density. Thus, we will compare our marking densities to this set of *violence data*.

The second set of data we have to evaluate our model gives the locations of where known or suspected gang members were stopped by the police. In such encounters, the officer fills out a Field Interview (FI) card, listing information about where the interaction took place and all individuals involved. These encounters are not initiated by violent events, and so we assume that these data are a sample of the gang densities, $u^{(i)}$. This data set of 1,669 events, covering the year of 2009, will be referred to as *FI data*. Both data sets can be seen in Figure 2. Due to the large number of gangs, only the aggregated data will be displayed here.

There is a possibility of errors in any data set, including inaccuracies, incompleteness, under-reporting of events, and bias [11]. Furthermore, for the data sets we are using, we should be cautious in the expectation that $p^{(i)}$ fully approximates the violence data and $u^{(i)}$ fully approximates the FI data. The nature of the sampling frame for the FI data is not perfectly understood, and there may be significant under-reporting of all but the most serious violent crimes. Nevertheless, it is reasonable to assume that a large number of these events can be predicted by the densities obtained by the model.

Another potential issue to consider is the difference in time frames for each set of data. The locations of the set spaces were taken from [28] published in 2010. Some set spaces may have moved during the eight years after the violence data was collected. As cities are ever changing, gangs may have adapted to the altered environments. For example, one housing area was redeveloped, forcing several Cuatro Flats gang members to relocate. This caused the gang to ultimately have two set spaces. For simplicity, we will only use the original set space in our model implementation.

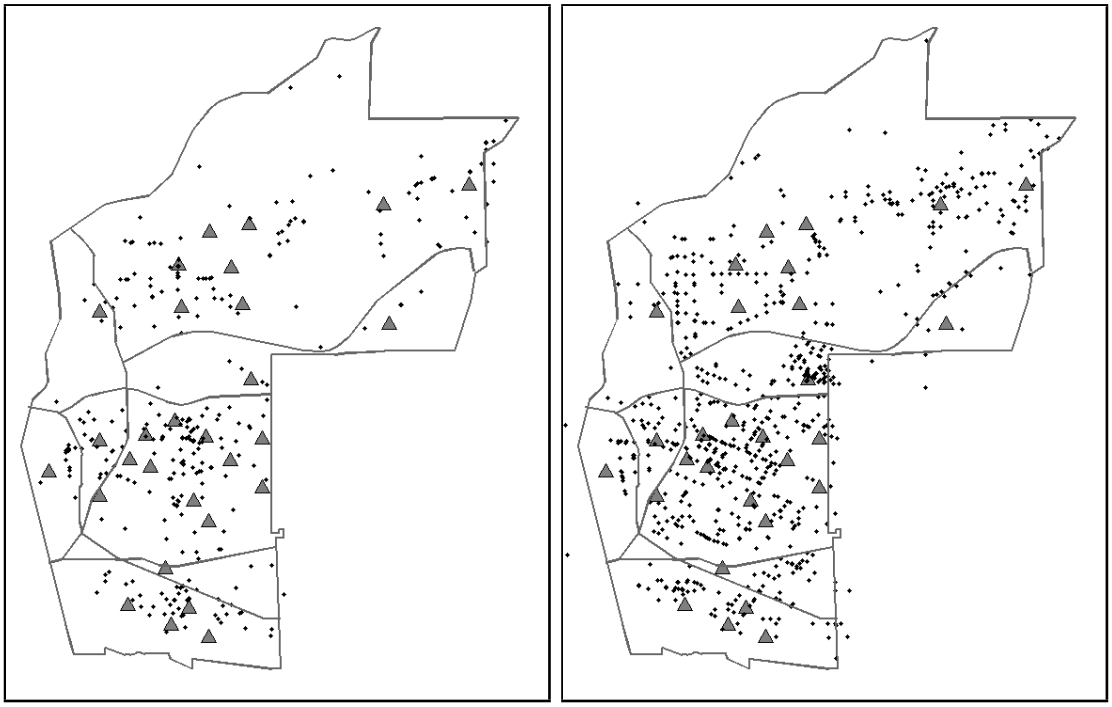

Figure 2: Violence and FI data in Hollenbeck. The set spaces are given by solid triangles in both images. The gang violence data (Left) and FI data (Right) are given by solid circles.

6 Results

With this implementation of the model for the Hollenbeck gangs, we optimize the parameters with respect to the rivalry network. Additionally, we must ensure that the parameter m is large enough to produce a marking density that is not nearly identical to the gang density. Listed in Table 1 are the parameters used for this analysis.

Parameter	Value
m	100
β	1
α	-1
Δt	0.001

Table 1: Parameter choices for the territory animal model.

We first compare our simulated network with that of the agent-based approach of [16] in Section 6.1. From here, we investigate the resulting gang and marking densities in Section 6.2. Given these densities, Section 6.3 estimates gang territory locations. One standard method for partitioning a region is through Voronoi diagrams, which we further discuss in Section 6.4. We then use the estimated territories to investigate the relationship with the two data sets in Section 6.5. Finally, we examine pairs of rival gangs and the locations of events with respect to the theoretical territories in Sections 6.6 and 6.7.

6.1 Rivalry Networks

To create a rivalry network from the territory animal model, we must determine what quantifies a rivalry. If the violence among gangs in Hollenbeck is primarily attributed to territorial issues, then we would expect a rivalry to exist if the densities of two gangs sufficiently overlap. We thus threshold the densities to produce an approximate territory, and then find the overlapping area between pairs of territories. Since there are 69 empirically known rivalries among the gangs in Hollenbeck, we select the top 69 area pairs to construct a network. The resulting rivalry network obtained from the simulation is given in Figure 3, together with the observed network and the Simulated Biased Lèvy walk Network (SBLN) obtained in [16].

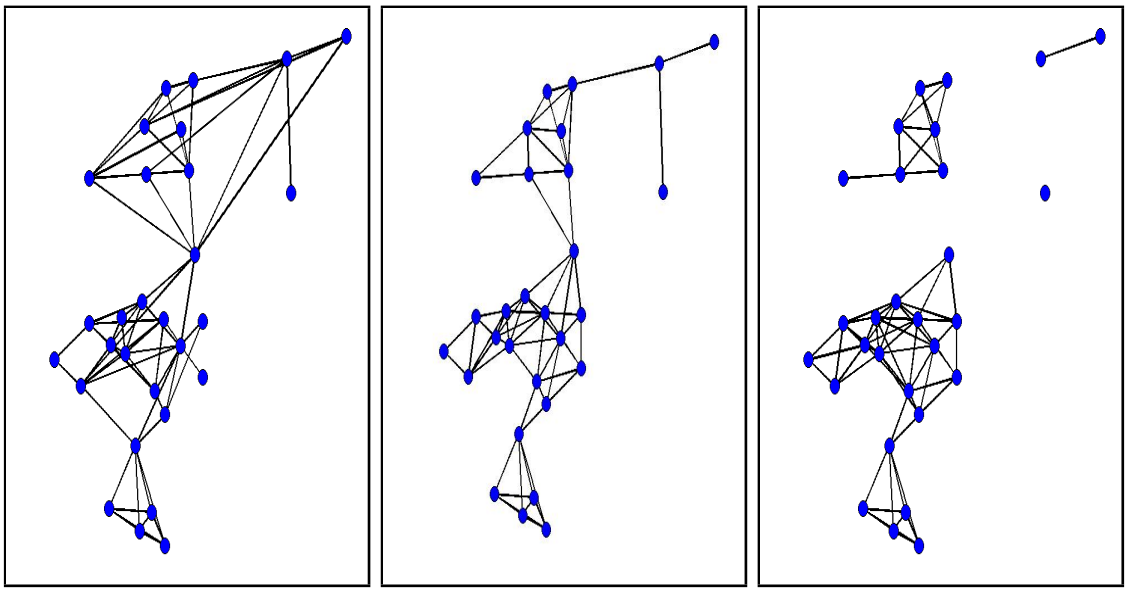

Figure 3: Comparison of rivalry networks. Each node in the network represents a gang's set space. An edge in the graph exists if there is a rivalry between the two gangs. The observed network (Left) is plotted with both the SBLN network from [16] (Middle) and the territory animal model from this paper (Right).

We notice that the territory animal model correctly identifies 45 of the 69 edges in the observed network. Additionally, this simulated network has similar graph properties with both of the other networks. To better quantify this similarity, we examine a few graph metrics that were previously used in [16].

We would like to inspect the accuracy of the simulated network. Initially, we calculate the number of true positives (TP), true negatives (TN), false positives (FP), and false negatives (FN). An edge is considered a true positive when it is correctly identified as an existing edge in the model and is present in the observed network, and it is a true negative when it is correctly identified as not being an edge. Alternatively, an edge is marked as a false positive if the simulation identifies it as an edge when it is not present in the observed network, and it is a false negative if the simulation fails to label a true rivalry as an edge. From these we calculate the *accuracy* score

$$ACC = \frac{TP + TN}{FP + FN + TP + TN}.$$

This value should fall between 0 and 1, with higher values indicating a more accurate graph. These values are presented in Table 2.

	TP	TN	FP	FN	ACC
Hegemann et al. SBLN	50	320	17	19	0.9113
Territory Animal Model	45	313	24	24	0.8818

Table 2: Accuracy measures for the Hegemann et al. SBLN model and the territory animal model.

While these accuracy measures are important, we would also like our rivalry network to have similar graph properties as the observed network. For example, the number of rivals that a gang has should be approximately the same in the simulation. Thus, we investigate features of the network related to the degree of a node $d(i)$, representing the number of rivals of a gang i. Three measures we use are the *graph density*, *degree variance*, and *Freeman's centrality measure*. Given G gangs, these are defined in [14, 35] as

$$\begin{aligned}
\text{Density} &= \frac{1}{G(G-1)} \sum_{i=1}^{G} d(i), \\
\text{Degree Variance} &= \frac{1}{G} \sum_{i=1}^{G} \left[d(i) - \left(\frac{1}{G} \sum_{j=1}^{G} d(j) \right) \right]^2, \\
\text{Centrality} &= \frac{1}{(G-1)(G-2)} \sum_{i=1}^{G} \left[\left(\max_j d(j) \right) - d(i) \right].
\end{aligned}$$

The density of the graph is a scalar multiple of the average degree. Thus, if two graphs have the same number of edges, then they will have the same density. The degree variance provides information on the spread of the degrees. Thus, a larger degree variance indicates a wider range of degrees, which translates to a larger spread in the number of rivals of each gang. The centrality measures whether there are key gangs that are more connected than the rest, indicating they are more central to the network. If all gangs have the same degree, i.e. no gang is more influential to the network, then the centrality measure would be zero. Alternatively, if one gang is connected to every other gang, and these are the only edges in the graph, then the network would have a high centrality measure.

These graph shape measures for the observed network, the Hegemann et al. SBLN network, and the territory animal model network are shown in Table 3. We note that the three networks have close values for the three metrics.

While it is of interest to compare the rivalry network from the territorial animal model to the observed network and the ones existing in the literature, we must also recognize that the method for obtaining the rivalry network from overlapping densities has limitations. More specifically, the edges that cross boundaries in the upper portion of the region are absent. This is expected since the model limits the smoothing of the gang densities across these boundaries. Thus, we do not anticipate much overlap in the territories of gangs in separate regions. Hence, we should examine other features of the model to determine the validity of the model.

	Density	Degree Variance	Centrality
Observed Network	0.16995	4.32105	0.20106
Hegemann et al. SBLN	0.16503	3.54578	0.16799
Territory Animal Model	0.16995	5.70036	0.16270

Table 3: Graph metrics comparing the observed network with the Hegemann et al. SBLN model and the territory animal model.

6.2 Marking and Gang Densities

Modeled gang and marking densities display some promising features. First, the gang densities $u^{(i)}$ remain centrally located about the known set spaces, with minimal overlap between gangs. Geographic boundaries limit the spread of gang density. Marking densities are highest between adjacent gangs that have a relatively small distance between them. Otherwise, the marking densities mimic the gang densities. This is expected as the steady-state solution of Equation (2) is given by

$$p^{(i)} = u^{(i)} \left[1 + m \sum_{j \neq i}^{n} p^{(j)} \right]$$

The plots of all gang and marking densities are provided together in Figure 4.

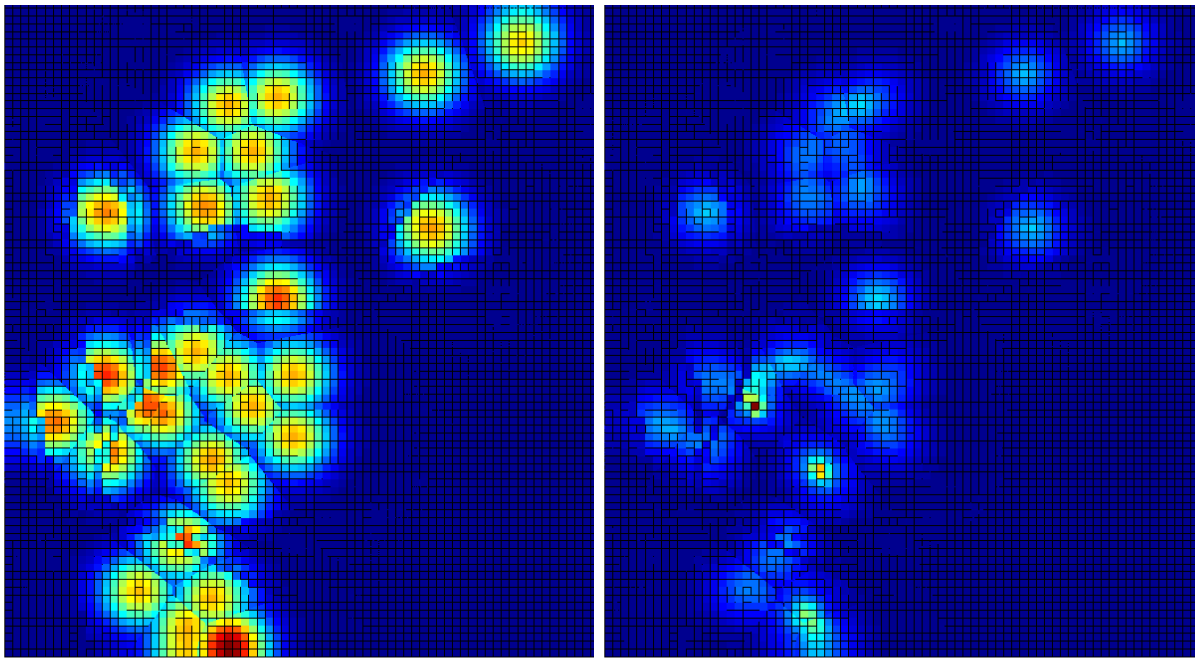

Figure 4: Simulated gang (Left) and marking (Right) densities in Hollenbeck. The densities for all of the gangs are plotted together. Red indicates a higher density and blue a lower density. The gang densities demonstrate the formation of territories and the impact of boundaries within the region. The marking densities are the highest between two close set spaces. Otherwise, the marking densities are similar to the gang densities.

To better demonstrate the impact of the semi-permeable boundaries that represent the major roads and the river, the gang density for a central gang is shown in Figure 5. The

set space for this particular gang is situated between two major freeways. To illustrate the impact of the southern boundary, we view the density facing East. Notice the dramatic drop in density over the boundary. Additionally, we see that some density still flows beyond the freeway as expected, since movement is not prohibitted across boundaries, only discouraged.

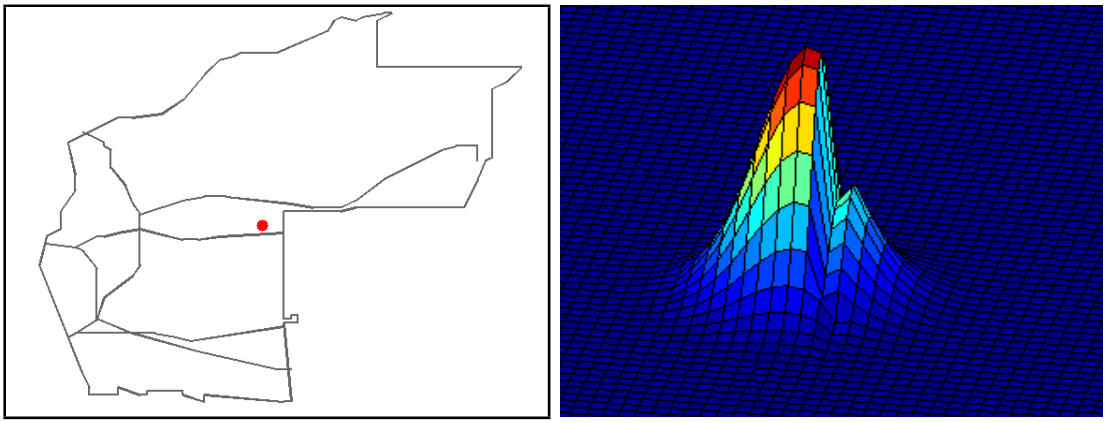

Figure 5: Impact of boundary on gang densities. The gang density (Right) for a gang with set space located between large freeways (Left) is illustrated here. The density image is facing East to demonstrate the impact of the southern boundary.

6.3 Territories

The ability to approximate gang territories is a desirable feature of this model. To do this, we classify a point (x, y) in space as belonging to the territory of gang i if

$$\begin{aligned} u^{(i)}(x,y) &> u^{(j)}(x,y) \qquad \text{for all } j \neq i \\ u^{(i)}(x,y) &> \delta. \end{aligned}$$

Using this thresholding with δ, we limit the size of the territories so they do not cover the entire region. We took $\delta = 0.001$. The case where $\delta = 0$ is discussed in Section 6.4. The resulting territories are shown together in Figure 6. Although the semi-permeable boundaries highly influence the gang densities, some territory plots seem to extend beyond these boundaries. This is particularly evident for the southern boundary of the gang plotted in Figure 5.

6.4 Voronoi Diagrams

Given a set of points, a Voronoi diagram partitions the area of interest into smaller regions that each contain only one of the points [13]. For a point x_A, we consider every pair (x_A, x_B) where $A \neq B$. We then construct a line between them that is equidistant to both points. After completing this for each point x_B, we take the resulting polygon that contains x_A. This is repeated for all points, decomposing the space into smaller regions. We compare the Voronoi diagram obtained from using the set spaces to the territories constructed with the territorial animal model. We obtain interesting results if we consider $\delta = 0$ instead of $\delta = 0.001$ (i.e. no thresholding of the densities). Figure 7 overlays the

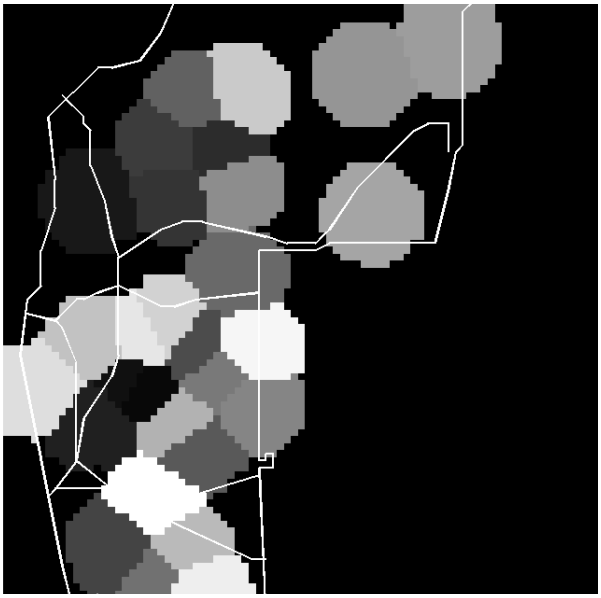

Figure 6: Estimated gang territories. The semi-permeable boundaries of the model and the county line are plotted over the territories in white.

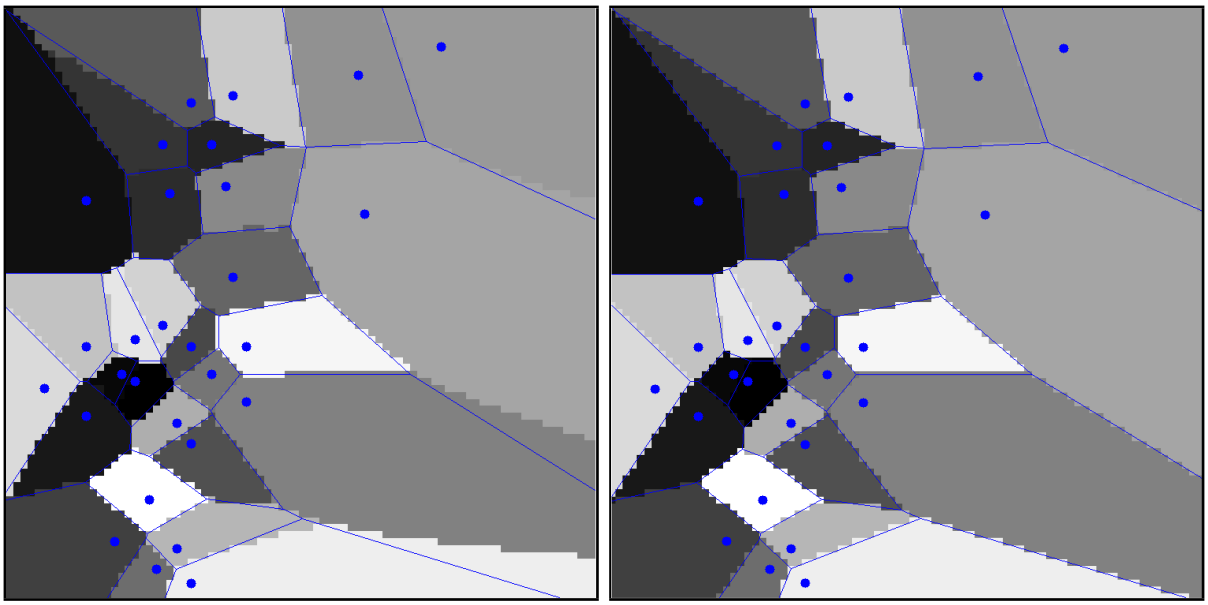

Figure 7: Voronoi plots compared to simulated territories. In both images, the set spaces for the gangs are represented by the solid circle. The solid lines give the Voronoi diagram for the region with input of the set spaces. The shaded regions provide the estimated gang territories with a Gaussian distribution for the gang densities (Right) and the $u^{(k)}$ gang densities obtained from the territory animal model (Left). Notice that the Gaussian distribution territories line up directly with the Voronoi plot, and the territory animal model only differs significantly on the far right portion of the region.

partitioning line segments of the Voronoi diagram on the constructed territories with no thresholding. We notice that they align almost exactly.

For comparison, we do a simple approximation to the gang densities by using a Gaus-

sian distribution centered at the set space. We used the parameter $\sigma = 3$ for the standard deviation of the distribution. Using the same technique for determining territories as above, we created a territory plot with no thresholding and plotted the Voronoi diagram over it as well. This is also shown in Figure 7. The boundaries of the territories match up exactly with the Voronoi diagram.

We notice the two territory plots and the Voronoi diagram are very similar. This suggests that the territories created using the territory animal model produces territories similar to using a standard normal distibution about the set space. However, we note that the normal distributions of separate gangs has significantly more overlap than the territory animal model gang densities. This does not show in these images as we only indicate which gang has a higher density here.

6.5 Comparison of Model Densities with Data

As discussed in Section 5, we have two data sets with which we will compare our model output. The FI data provides the locations of where individuals have been stopped by the police. We assume this to be a reasonable sample of the gang densities. Thus, we plot the FI data over the gang densities in Figure 8. Additionally, we have violence data for interactions between gangs. These events are most likely to occur in locations where the marking density is high. Therefore, we plot this data over the marking densities in Figure 8.

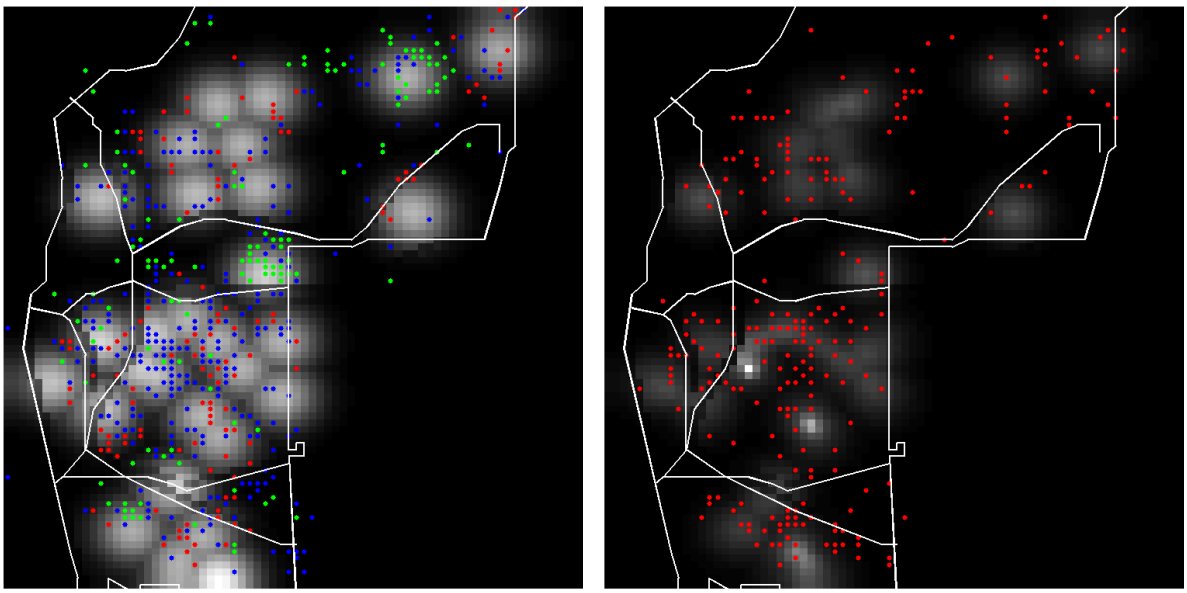

Figure 8: Data points and the simulated densities. The gang densities and the FI data are plotted together (Left), and the marking densities are given with the violence data (Right). Here, the densities are provided as the background grayscale image with whiter colors representing higher values. In the FI data image (Left), the green dots are for individuals in their own theoretical territory, the red dots are for individuals in their rival gang's theoretical territory, and the blue dots are for the other cases.

To see how well the model fits the data, we examine the log-likelihood of the events. The results are given in Table 4. In addition to the log-likelihood of events with the territorial animal model, we examine the Gaussian distribution model. We find that

the territorial animal model performs better than the Gaussian distribution model when $\sigma = 3$, the standard deviation used in Figure 7. We optimized the σ to give the best log-likelihood, resulting in a value of $\sigma = 11.5$. However, theoretical territory plots for this value resulted in gangs having set spaces in other gangs' theoretical territories. This is an undesirable property, which is why the image is not included in the paper, but we include the log-likelihood in the table for comparison.

Method	Data Set	Log-likelihood
Territorial Animal Model	FI Data	-15572
Territorial Animal Model	Violence Data	-5260
Gaussian Distribution Model ($\sigma = 3$)	FI Data	-20755
Gaussian Distribution Model ($\sigma = 11.5$)	FI Data	-9102.4

Table 4: Log-likelihood of events for the territorial animal model and the Gaussian distribution model. For the Gaussian distributions, we use $\sigma = 3$ as in Section 6.4 and $\sigma = 11.5$. The latter value gives the best log-likelihood, but creates territories that does not contain the set spaces for some gangs.

Overall, we notice some interesting properties of the locations of the individuals in the FI data. Figure 8 plotted these data in different colors to correspond to the various cases. In particular, green dots represent gang members that are located in their own theoretical territory as estimated in Figure 6. The red dots show gang members located in a rival gang's theoretical territory, and the blue dots represent individuals that are neither in their own territory nor a rival gang's territory. Here, we determine a rival gang from the observed rivalry network. To help examine the individual cases, we plot them separately in Figure 9. We notice that the data points corresponding to locations

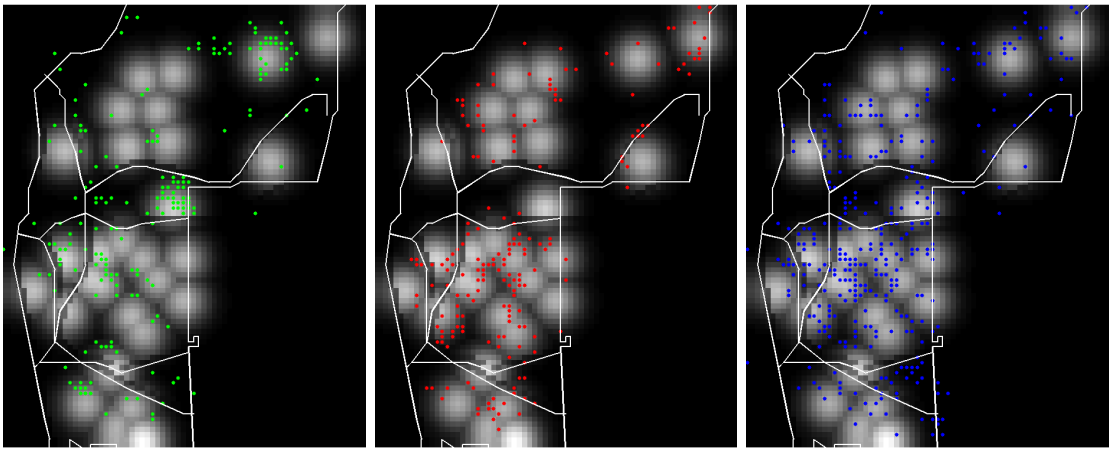

Figure 9: FI data plotted over the gang densities determined by the territorial animal model. The gang members in their own theoretical territories (Left), the gang members in their rival's theoretical territory (Middle), and the other cases (Right) are plotted here. A dot represents a location where a gang member was found. The grayscale image in the background shows the gang densities estimated by the territorial animal model.

where the gang members are not in their own theoretical territory are more likely to

occur in areas near the boundaries of other gangs' theoretical territories. Perhaps these individuals were passing through the region by slipping between territories.

We highlight the FI data for three individual gangs in Figure 10. We notice that the densities visually indicate where to find the majority of the gang members. Instances where the individuals are not in the general vicinity of the home territory often occur near the major roads.

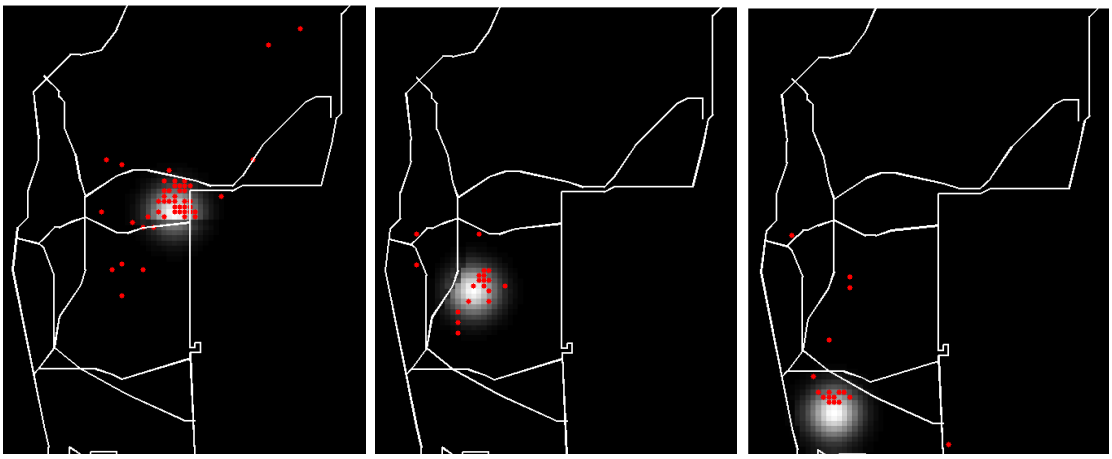

Figure 10: FI data for three individual gangs. The red dots indicate the position of where a gang member was located. The grayscale image provides the gang's density information estimated by the territorial animal model.

Next, we examine the violence data and how it compares to the theoretical marking densities produced by the model. Table 4 provides the log-likelihood information for the locations of events given a particular gang. Since we do not have another model to compare this with, we instead flag a certain portion of the city and find how many events occurred in this region. More specifically, we take all points such that for any i,

$$p^{(i)}(x,y) > \gamma \cdot \max_{j,x,y} \left(p^{(j)}(x,y)\right).$$

We took γ to be $0.2, 0.1$, and 0.05. The flagged regions are shown in Figure 11, and more information on the results are provided in Table 5. By flagging less than 14% of the cells, we predict more than half of the data.

γ	Percent of City Flagged	Percent of Violence Data Predicted
0.2	5.02%	20.61%
0.1	13.94%	50.91%
0.05	22.46%	71.21%

Table 5: Proportion of data predicted given a flagged region of the city.

6.6 Rival Gang Territories and Events

Given approximate territories for gangs, we can investigate the locations of events with respect to these regions. Figure 12 gives the theoretical territories of three sets of rival

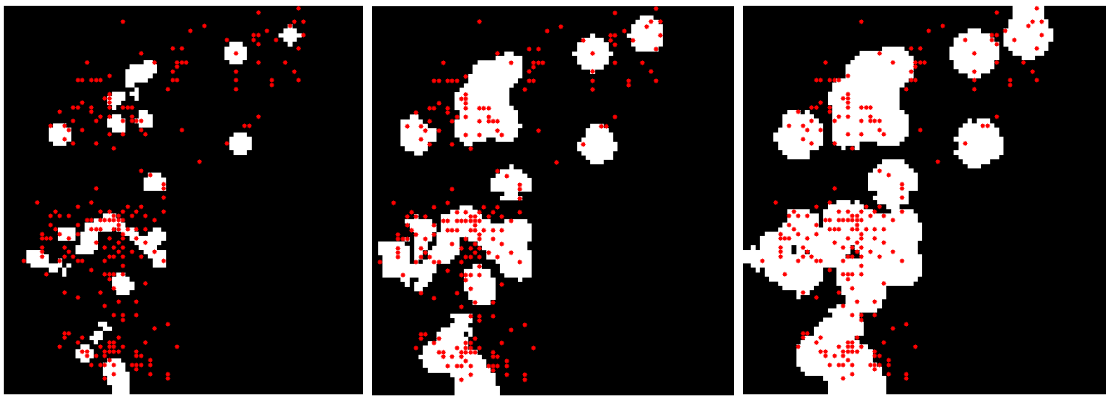

Figure 11: Violence data compared to flagged regions of the city. From left to right, we have $\gamma = 0.2, 0.1, 0.05$. The red dots indicate locations of violence between two gangs. The white regions are the flagged cells of the marking densities where we expect the events are more likely to occur.

gangs and the locations of the known violent interactions between them. Since we have information about which gang is the suspect and which is the victim, we illustrate which gang is the victim by matching the interior color of the marker with the territory color. In these three rivalries, we notice that all events occur near the boundaries of the theoretical territories. Events slightly to the interior of the theoretical territory boundary correspond with victim gangs in their own territory.

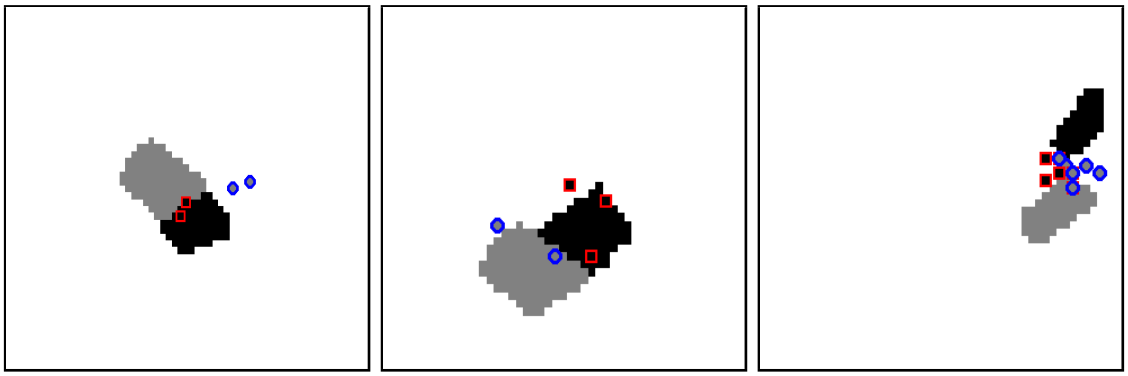

Figure 12: Territories and events of rival gangs. The three plots represent three pairs of rival gangs and the violent interactions between them. The interior color of the markers (circles and squares) indicates which gang is the victim by matching the color of its theoretical territory. All events occur near the boundaries of the territories.

Sometimes there exists a rivalry between gangs of varying sizes. One such pair is illustrated in Figure 13, with one gang significantly larger than the other. Counterintuitively, the gang with the black set space is the larger gang and has a much greater number of events where it is the victim. We also notice that the smaller gang is only the victim on the boundary of the larger gang's theoretical territory or on the interior of its own theoretical territory. Since this data was recorded, the smaller gang collapsed after a key gang member was killed. Thus, the smaller number of attacks by the larger gang may have had more impact than the larger number made by the smaller gang.

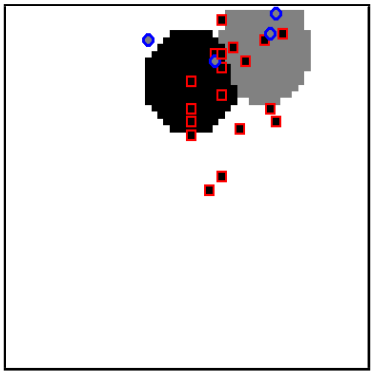

Figure 13: A rival pair of gangs with different sizes. The larger gang, whose theoretical territory is in black, is significantly larger than the smaller gang. The smaller gang is only the victim on the boundary of the larger gang's territory or on the interior of its own territory.

6.7 Suspect Versus Victim

In the previous section, we noticed a pattern where the locations of events occur with respect to theoretical territory boundaries. Figure 14 shows six pairs of rival gangs and where their violent interactions occurred. We notice a trend where the events typically fall either near the boundary of the approximated territories of either gang, on the interior of the victim's territory, or are far from either theoretical territory.

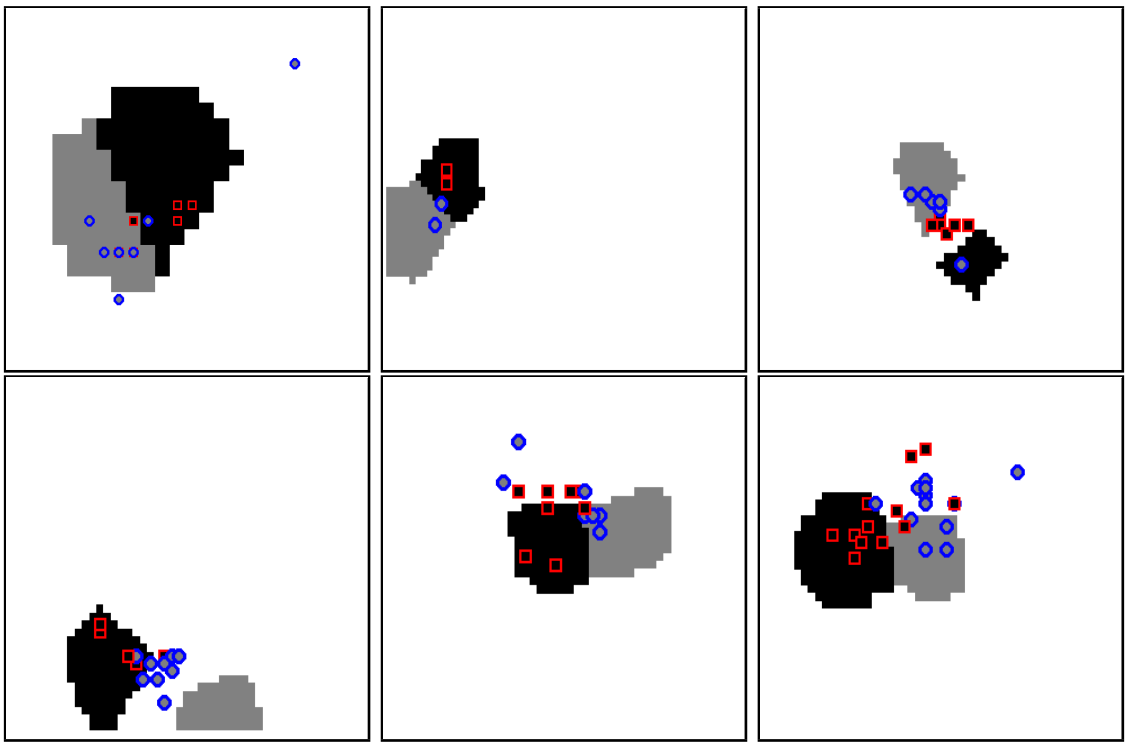

Figure 14: Rival gang territories and the events between them. The victim's gang's theoretical territory color matches the interior of the marker. The majority of events occur near the approximate territory boundaries, on the interior of the victim's territory, or away from both territories.

With this observation, we consider the location of events with respect to the bound-

aries of the approximate territories for both the suspect and the victim gangs. Previously, the authors of [6] investigated the positioning of the events with respect to a boundary line between gangs, equidistant to both set spaces. With the theoretical boundaries from the territorial animal model, we are able to further analyze this data with respect to all boundaries. Given the victim gang's theoretical territory, we find the distance from an event to the territory boundary. We let this value be negative if the event occurs in the victim's territory and positive if it is outside. A histogram of these distances is provided in Figure 15. We see that the events strongly cluster near the boundary of the victim.

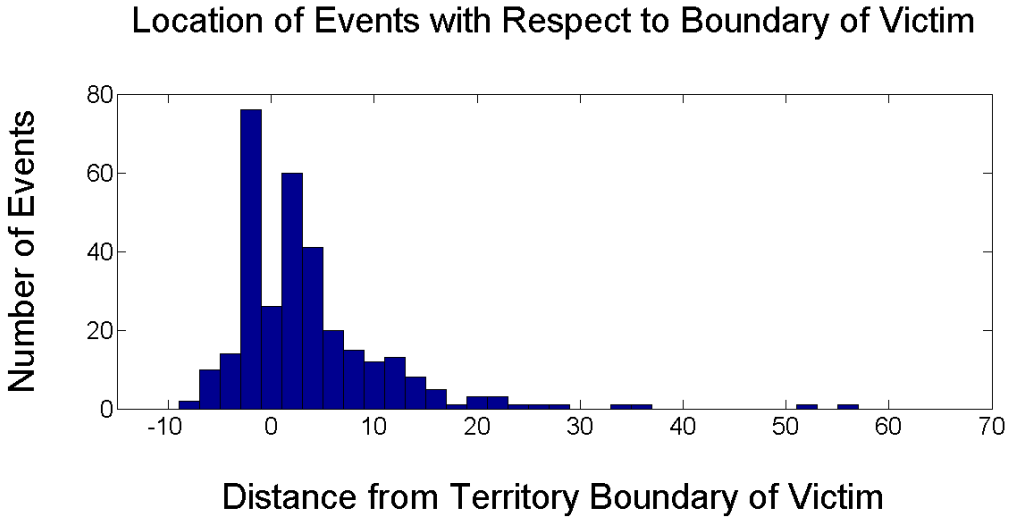

Figure 15: Histogram of the distance of an event to the boundary of the victim's theoretical territory. Negative values indicate the event occurred on the interior of the victim's territory, and positive values are for events on the exterior of the region. The distance is the number of grid units to the closest boundary point.

We also note that the distribution is slightly skewed to have a larger number of events just interior to the victim's territory. This agrees with our observation in Figure 14.

Since the rival gangs are not necessarily adjacent to each other, we also repeat this analysis for the location of events with respect to the suspect's theoretical territory. Again, negative values indicate the event occurs on the interior of the suspect's territory, and positive values for the outside. The histogram is included in Figure 16. From this figure, we observe that the majority of events occur near the boundary of the suspect's territory, but skewed to the exterior of the region.

Quantitatively, we find 24.7% of the events occur within three grid units of the theoretical boundaries of both suspect and victim gangs. Additionally, 66.8% of the events occur within three grid units of either the suspect or victim gang's territory boundary.

7 Discussion

Using the framework of the coyote model proposed in [24], we formulated a model for street gang spatial behavior. This model was able to incorporate spatial features of the region that limit the movement individuals across these semi-permeable boundaries. For

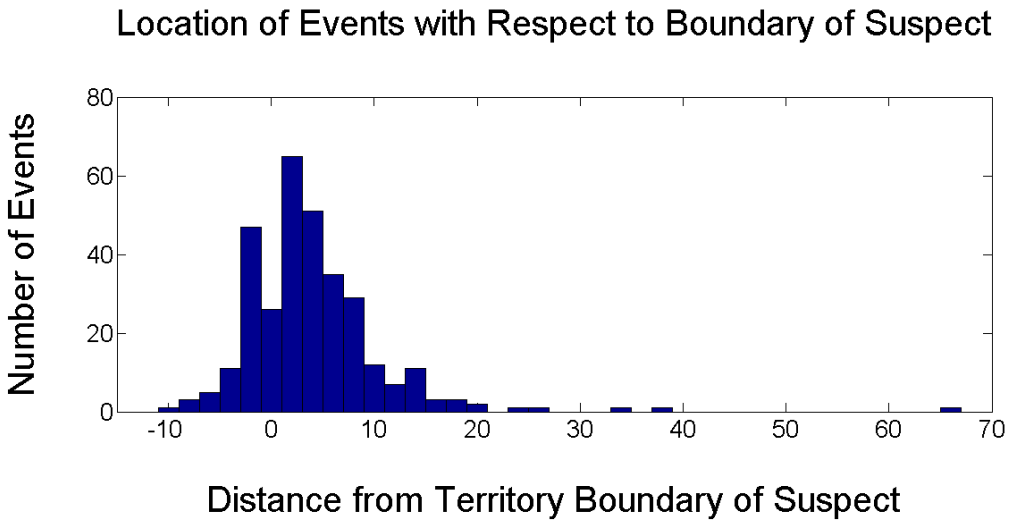

Figure 16: Histogram of the distance of an event to the boundary of the suspect's theoretical territory. Negative values indicate the event occurred on the interior of the suspect's territory, and positive values are for events on the exterior of the region. The distance is the number of grid units to the closest boundary point.

each gang, the model produced a gang density and marking density, indicating where gang members are expected to be and where their tags are most likely to be found.

As a first approach to evaluating our model, we compared the rivalry network from our model to the oberseved network and the Hegemann et al. SBLN network. While our model's network gave similar metric values, it did not outperform the SBLN network. This is due to the fact that we constructed the rivalry network from overlapping gang densities, which are discouraged from spreading beyond the semi-permeable boundaries encoded in the model. Thus, rivalries that cross these boundaries are not likely to be captured by the method we used to produce a network. However, this method is able to provide more information than just a rivalry network. In particular, it can be used to approximate gang territories and the locations of violent interactions.

From the gang densities produced by the model, we approximated gang territories by classifying a point based on which gang has the highest density at that location. Without any thresholding, the resulting territory plot closely approximates a Voronoi diagram. With thresholding, the resulting territory plots give reasonable estimates for each gang's turf.

By flagging the cells with the highest theoretical marking densities, we were able to identify the majority of the violent events with a small portion of the city. Additionally, we were able to identify interesting behaviors of rival gangs. Events were more likely to occur in the interior of the victim gang's theoretical territory or on the boundary of either the victim or suspect gang's theoretical territory.

While comparing the gang densities to the FI data, we found the gang members were often not in the general vicinity of their approximated home territory. These individuals were frequently traveling on the boundaries of other gang's territories. Despite this, we demonstrated with three gangs that we were still able to give a good density estimate to the location of gang members.

As a next step in this modeling approach, we would like to include the gang sizes in the model. We would expect gangs with more individuals to produce more taggings and require more space. Additionally, we would like to incorporate other features that might impact the territory locations, such as police stations or multiple set spaces.

8 Acknowledgements

We would like to thank Martin Short for helpful conversations. This work was sponsored by AFOSR MURI grant FA9550-10-1-0569, NSF grant DMS-0968309, NSF grant DMS-0907931, ARO grant W911NF1010472, reporting number 58344-MA, ONR grant N000141010221, and ARO-MURI award W911NF-11-1-0332.

References

[1] A. Alonso. Urban graffiti on the city landscape. *University of Southern California*, 1998.

[2] E. Anderson. *Code of the Street: Decency, Violence, and the Moral Life of the Inner City*. W. W. Norton & Company, Inc., 2000.

[3] J. Austin, E. Smith, S. Srinivasan, and F. Sanchez. Social dynamics of gang involvement: A mathematical approach. *Mathematical and Theoretical Biology Institute, MTBI-08-08M*, 2011.

[4] A. Barbaro, L. Chayes, and M. R. D'Orsogna. Territorial development based on graffiti: a statistical mechanics approach. 2011.

[5] J. Bascompte and R. V. Sole, editors. *On wolf territoriality and deer survival*. Springer - Verlag, 1998.

[6] P. Brantingham, G. Tita, M. Short, and S. Reid. The community context of gang territorial boundaries. 2011.

[7] B. Briscoe, M. Lewis, and S. Parrish. Home range formation in wolves due to scent marking. *Bulletin of Mathematical Biology*, 64:261–284, 2002. 10.1006/bulm.2001.0273.

[8] W. Brown. Graffiti, identity and the delinquent gang. *Internal Journal of Offender and Comparative Criminology*, 22(1):46–48, 1978.

[9] S. H. Decker and B. Van Winkle. *Life in the Gang: Family, Friends, and Violence*. Cambridge University Press, 1996.

[10] P. K. Eason, G. A. Cobbs, and K. G. Trinca. The use of landmarks to define territorial boundaries. *Animal Behaviour*, 58(1):85 – 91, 1999.

[11] J. Eck and L. Liu. Contrasting simulated and empirical experiments in crime prevention. *J. Exp. Criminol.*, 2008.

[12] M. Egesdal, C. Fathauer, K. Louie, and J. Neuman. Statistical modeling of gang violence in Los Angeles. *SIAM Undergrad. Res. Online*, 3, 2010.

[13] S. Fortune. Voronoi diagrams and Delaunay triangulations. In D. Du and F. Hwang, editors, *Computing in Euclidean Geometry*, volume 4 of *Lecture Notes Series on Computing*, pages 225–236. World Scientific, 1995.

[14] L. C. Freeman. Centrality in social networks conceptual clarification. *Soc. Netw.*, 1(3):215 – 239, 1978-1979.

[15] M. B. Gordon. A random walk in the literature on criminality: A partial and critical view on some statistical analyses and modelling approaches. *Eur. J. Appl. Math.*, 21(Special Double Issue 4-5):283–306, 2010.

[16] R. A. Hegemann, L. M. Smith, A. B. Barbaro, A. L. Bertozzi, S. E. Reid, and G. E. Tita. Geographical influences of an emerging network of gang rivalries. *Physica A: Statistical Mechanics and its Applications*, 390(21-22):3894 – 3914, 2011.

[17] E. Holmes, M. Lewis, J. Banks, and R. Veit. Partial differential equations in ecology: Spatial interactions and population dynamics. *Ecology*, 75(1):17–29, 1994.

[18] S. R. Jammalamadaka and A. SenGupta. *Topics in Circular Statistics*, volume 5 of *Multivariate Analysis*. World Scientific Publishing Co. Pte. Ltd., 2001.

[19] J. E. Jankowski, S. K. Robinson, and D. J. Levey. Squeezed at the top: Interspecific aggression may constrain elevational ranges in tropical birds. *Ecology*, 91(7), 2010.

[20] M. A. Lewis and J. D. Murray. Modelling territoriality and wolf-deer interactions. *Nature*, 366, 1993.

[21] M. A. Lewis, K. A. J. White, and J. D. Murray. Analysis of a model for wolf territories. *Journal of Mathematical Biology*, 35:749–774, 1997. 10.1007/s002850050075.

[22] D. Ley and R. Cybriwsky. Urban graffiti as territorial markers. *Ann. Assoc. Am. Geogr.*, 64(4):491–505, 1974.

[23] P. Moorcroft, M. Lewis, and R. Crabtree. Home range analysis using a mechanistic home range model. *Ecology*, 80:1656 – 1665, 1999.

[24] P. R. Moorcroft, M. A. Lewis, and R. L. Crabtree. Mechanistic home range models capture spatial patterns and dynamics of coyote territories in yellowstone. *Proceedings: Biological Sciences*, 273(1594):1651–1659, 2006.

[25] J. Moore. *Going down to the barrio: Homeboys and homegirls in change*. Temple University Press, 1991.

[26] R. P. Peters and L. D. Mech. Scent-marking in wolves: Radio-tracking of wolf packs has provided definite evidence that olfactory sign is used for territory maintenance and may serve for other forms of communication within the pack as well. *American Scientist*, 63(6):pp. 628–637, 1975.

[27] Product No. 2009-M0335-001. National gang threat assessment. *Natl. Gang Intell. Cent.*, January 2009.

[28] S. Radil, C. Flint, and G. Tita. Spatializing social networks: Using social network analysis to investigate geographies of gang rivalry, territoriality, and violence in Los Angeles. *Ann. Assoc. Am. Geogr.*, 100(2):307–326, 2010.

[29] M. Short, G. Mohler, P. Brantingham, and G. Tita. Gang rivalry dynamics via coupled point process networks. 2011.

[30] A. Stomakhin, M. Short, and A. Bertozzi. Reconstruction of missing data in social networks based on temporal patterns of interactions. *Inverse Problems*, 27(11):115013, 2011.

[31] T. A. Taniguchi, J. H. Ratcliffe, and R. B. Taylor. Gang set space, drug markets, and crime around drug corners in Camden. *Journal of Research in Crime and Delinquency*, 48(3):327–363, Aug. 2011.

[32] F. M. Thrasher. *The Gang: A Study of 1313 Gangs in Chicago.* University of Chicago Press, 1927.

[33] G. Tita, J. Cohen, and J. Engberg. An ecological study of the location of gang "set space". *Soc. Probl.*, 52(2):272–299, 2005.

[34] G. Tita, K. Riley, G. Ridgeway, C. Grammich, A. Abrahamse, and P. Greenwood. Reducing gun violence: Results from an intervention in East Los Angeles. *Natl. Inst. Justice, RAND*, 2003.

[35] S. Wasserman and K. Faust. *Social Network Analysis: Methods and Applications.* Cambridge University Press, 2009.

[36] D. P. Watts and J. C. Mitani. Boundary patrols and intergroup encounters in wild chimpanzees. *Behaviour*, 138(3):299–327, 2001.

[37] K. White, M. Lewis, and J. Murray. A model for wolf-pack territory formation and maintenance. *Journal of Theoretical Biology*, 178(1):29 – 43, 1996.